





Original Research

Long-Range Projections of Cortical GABAergic Neurons to the Midline Dorsal Thalamic Nuclei in GAD67-GFP Mice

Yi-Yao Li¹, Fei Li¹, Ming-Ming Zhang^{1,*}, Yun-Qing Li^{1,2,3,*}

¹Department of Anatomy, Histology and Embryology & K. K. Leung Brain Research Centre, The Fourth Military Medical University, 710032 Xi'an, Shaanxi, China

²Department of Human Anatomy, Basic Medical College, Zunyi Medical University, 563006 Zunyi, Guizhou, China

³Department of Anatomy, Basic Medical College, Dali University, 671000 Dali, Yunnan, China

*Correspondence: mmzhang@fmmu.edu.cn (Ming-Ming Zhang); deptanat@fmmu.edu.cn (Yun-Qing Li)

Academic Editor: Changjong Moon

Submitted: 9 October 2025 Revised: 16 November 2025 Accepted: 25 November 2025 Published: 26 December 2025

Abstract

Background: Cortical γ -aminobutyric acidergic (GABAergic) neurons are characterized primarily as local inhibitory interneurons that modulate cortical pyramidal neuronal activity. However, emerging evidence has demonstrated that some of them may project to subcortical structures, such as the midline dorsal thalamic nuclei (MDTN), which play a pivotal role in sensory information transmission and emotional regulation. The present study aimed to investigate whether cortical GABAergic neurons project to the MDTN. **Methods:** To address this question, this study combined retrograde tracing with immunofluorescent histochemical staining in GAD67-green fluorescence protein (GAD67-GFP) mice. **Results:** Cholera toxin B subunit (CTB) retrograde-labeled (CTB⁺), GAD67-GFP-immunoreactive (GAD⁺), and GAD and CTB double-labeled (GAD⁺+CTB⁺) neurons were identified across many cortical regions. CTB⁺ neurons were mainly observed in the motor cortices, cingulate cortex (Cg), prelimbic cortex (PrL), and insular cortex (IC) with sparse distributions in the sensory cortices, orbitofrontal cortex (OFC), piriform cortex (Pir) and claustrum (CL). GAD⁺ neurons were distributed throughout all cortical layers. In the sensory, motor, and granular insular cortices, the highest density was observed in layers II/III or V, with a relatively sparse distribution in layers I and IV. These layers were also widely distributed in other cortical regions such as the OFC, Cg, PrL, and Pir. GAD⁺+CTB⁺ neurons were mainly concentrated in layers V/VI of the motor, sensory, and IC cortices, with sparse distributions in the OFC, PrL, and Cg. These neurons spanned a rostrocaudal range of +2.34 mm to −0.46 mm from the bregma. Quantitative analysis showed that GAD⁺+CTB⁺ neurons accounted for 0.25%–0.55% of GAD⁺ neurons and 2.52%–4.93% of CTB⁺ neurons, respectively. **Conclusions:** The present results confirmed the existence of long-range GABAergic projections from the cortex to the MDTN and provide a morphological basis for the functional study of corticothalamic regulation through GABAergic projections.

Keywords: GABAergic neurons; cerebral cortex; midline thalamic nuclei; neuronal pathway tracing

1. Introduction

The mammalian cortex is a highly organized laminar structure composed of distinct layers, each of which contains specialized neuronal populations [1]. Cortical neurons are broadly classified into 2 types on the basis of their neurotransmitter phenotypes: glutamatergic excitatory neurons and γ -aminobutyric acidergic (GABAergic) inhibitory neurons. Glutamatergic pyramidal neurons are considered projection neurons with both local and long-range connections, whereas GABAergic neurons have traditionally been regarded as local interneurons that regulate cortical activity through both feedforward and feedback inhibitions [2,3]. These inhibitory interneurons are thought to lack the capacity for long-range projections instead forming local synaptic connections with pyramidal neurons to maintain the cortical excitation-inhibition balance [4,5].

However, growing evidences have revealed the existence of long-range GABAergic neurons (LRGNs) in the central nervous system (CNS) in multiple mammalian species [6]. Previous studies have demonstrated GABAer-

gic projections from the cat auditory cortex (AC) to both the contralateral AC and ipsilateral medial geniculate body [7], as well as from the rat hippocampus to the medial ambiguous nucleus [8]. Subsequent study identified the presence of callosal-projecting GABAergic neurons in the rat AC, showing that these LRGNs frequently target other GABAergic neurons to mediate long-range disinhibition [6]. Anatomical studies have localized cortical LRGNs predominantly in layers II/III and V/VI of sensory [9], motor [10], and association cortices [11], with axonal branches projecting to diverse subcortical regions, including the striatum and amygdala [12]. Long-range GABAergic projections also extend from the frontal cortex to multiple subcortical structures, including the caudate putamen, pallidum, nucleus accumbens, and midline dorsal thalamic nuclei (MDTN) [11]. These findings suggest that LRGNs represent a previously underappreciated component of cortical-subcortical pathways, potentially mediating complex forms of long-range inhibition.



The corticothalamic pathway is particularly relevant in the present study. The dorsal thalamus, particularly the MDTN, comprises the functionally distinct paraventricular thalamic nucleus (PVT), central medial thalamic nucleus (CM), and intermediodorsal thalamic nucleus (IMD), which serves as a critical hub for sensory integration and emotional processing [13]. The PVT is predominantly composed of excitatory neurons that regulate arousal, pain, feeding, addiction, reward, and fearful memory [14–16]. The IMD is an essential signal integration site within the cortico-thalamic reticular nucleus-thalamus tripartite pathway that specifically contributes to the regulation of fear-induced escape behavior [17]. The CM participates in regulating anesthesia and arousal, pain and itch sensation, emotional processing, and cognitive functions [18,19]. Corticothalamic projections to the MDTN subnuclei likely constitute distinct neural substrates for pain and itch transmission, emotional regulation, and cognitive control. Although glutamatergic corticothalamic projections have been extensively characterized, the GABAergic projections from the cortex to the MDTN remain poorly understood.

Glutamic acid decarboxylase (GAD), the sole rate-limiting enzyme that converts glutamate to GABA, exists in two isoforms: GAD67 (encoded by *GAD1*) and GAD65 (encoded by *GAD2*). GAD67 is constitutively expressed in virtually all GABAergic neurons, whereas GAD65 is primarily localized to specific synaptic terminals, making GAD67 a more comprehensive marker of GABAergic neurons [20]. In GAD67-green fluorescence protein (GAD67-GFP) knock-in mice, the *GFP* gene is inserted into the *GAD1* locus, allowing GFP expression under the control of the endogenous *GAD1* promoter. Consequently, all GAD67-expressing neurons exhibited green fluorescence, enabling specific and comprehensive visualization of GABAergic neurons [21].

In this study, we employed GAD67-GFP knock-in mice combined with immunofluorescence histochemical staining and retrograde tracing following the injection of cholera toxin B subunit (CTB) into the MDTN. This approach enabled us to map GABAergic projections from different cortical regions to the MDTN, thereby providing anatomical evidence for this understudied pathway and revealing its potential role in corticothalamic projections.

2. Materials and Methods

2.1 Animals

Eight adult male GAD67-GFP knock-in mice (8 weeks old, 20–25 g) were obtained by time-mating C57BL/6 wild-type mice with heterozygous GAD67-GFP knock-in mice. Two male heterozygous GAD67-GFP knock-in mice (JAX Stock #007677, Bar Harbor, ME, USA) were purchased from the Jackson Laboratory. The C57BL/6 mice were purchased from the Experimental Animal Center of the Fourth Military Medical University

(Xi'an, Shaanxi, China). The mice were housed under a 12/12 h light/dark cycle with free access to food and water.

2.2 Brain Stereotaxic Injection

Mice were anesthetized via an intraperitoneal (*i.p.*) injection of 40 mg/kg sodium pentobarbital (P3761, Sigma-Aldrich, St. Louis, MO, USA) dissolved in sterile saline and positioned on a stereotaxic apparatus (Model 68803, RWD Life Science, Shenzhen, Guangdong, China) for surgery. The scalp was shaved and disinfected with 70% ethanol (033361.M1, Thermo Fisher Scientific, Waltham, MA, USA) and betadine solution (395516, Ricca Chemical Company, Arlington, TX, USA). Following a midline incision, the skull surface was exposed and levelled using bregma and lambda landmarks. A total of 0.1 μ L of Alexa Fluor 594 conjugated cholera toxin B subunit (CTB-Alexa 594; C34777, Invitrogen, Carlsbad, CA, USA), used for retrograde neural tracing, was injected via a 1 μ L Hamilton microinjector (80100, Hamilton Company, Reno, NV, USA) equipped with a glass-tipped needle (internal tip diameter 15–25 μ m and outer diameter 20–30 μ m).

The microinjector was inserted into the MDTN of each mouse by obliquely advancing the needle from the hind-brain at a 30° angle to the vertical line to inject the CTB-Alexa 594 (Fig. 1A). The injection coordinates based on the mouse brain atlas [22] are defined as follows: AP, –2.08 mm; ML, 0.00 mm; DV, –4.16 mm. The injections were performed under pressure for 15 min, followed by a 5-minute diffusion period before needle retraction. After injection, the mice were maintained for a 10-day survival period to allow optimal retrograde transport of the tracer.

2.3 Brain Section Preparation

After being euthanized with an overdose of pentobarbital sodium (100 mg/kg, *i.p.*), the mice were perfused transcardially with 50 mL of cold 0.01 M phosphate-buffered saline (PBS, pH 7.4; P4474, Sigma-Aldrich) for blood clearance, followed by 150 mL of 4% (w/v) paraformaldehyde (8.18715, Sigma-Aldrich) in 0.1 M phosphate buffer (PB, pH 7.4; 17202, Millipore, Burlington, MA, USA) for fixation. The brains were carefully extracted and postfixed in the same fixative for 4 hours at 4 °C. The brains were subsequently transferred to 0.1 M PB (pH 7.4) containing 30% sucrose (S5016, Sigma-Aldrich) (w/v) overnight at 4 °C. The brains were coronally cut into 30- μ m-thick sections via a freezing microtome (CM1950, Leica, Heidelberg, Germany). The sections were serially collected in 4 dishes containing 0.01 M PBS (pH 7.4).

2.4 Histology and Immunofluorescent Histochemistry

Sections from the first dish were mounted onto clean glass slides (0317-2101, Citotest, Haimen, Jiangsu, China), and the extent of the CTB-Alexa 594 injection sites was examined via an epifluorescence microscope (BX-60, Olympus, Tokyo, Japan). Only the sections with accurate injection sites were selected for further study.

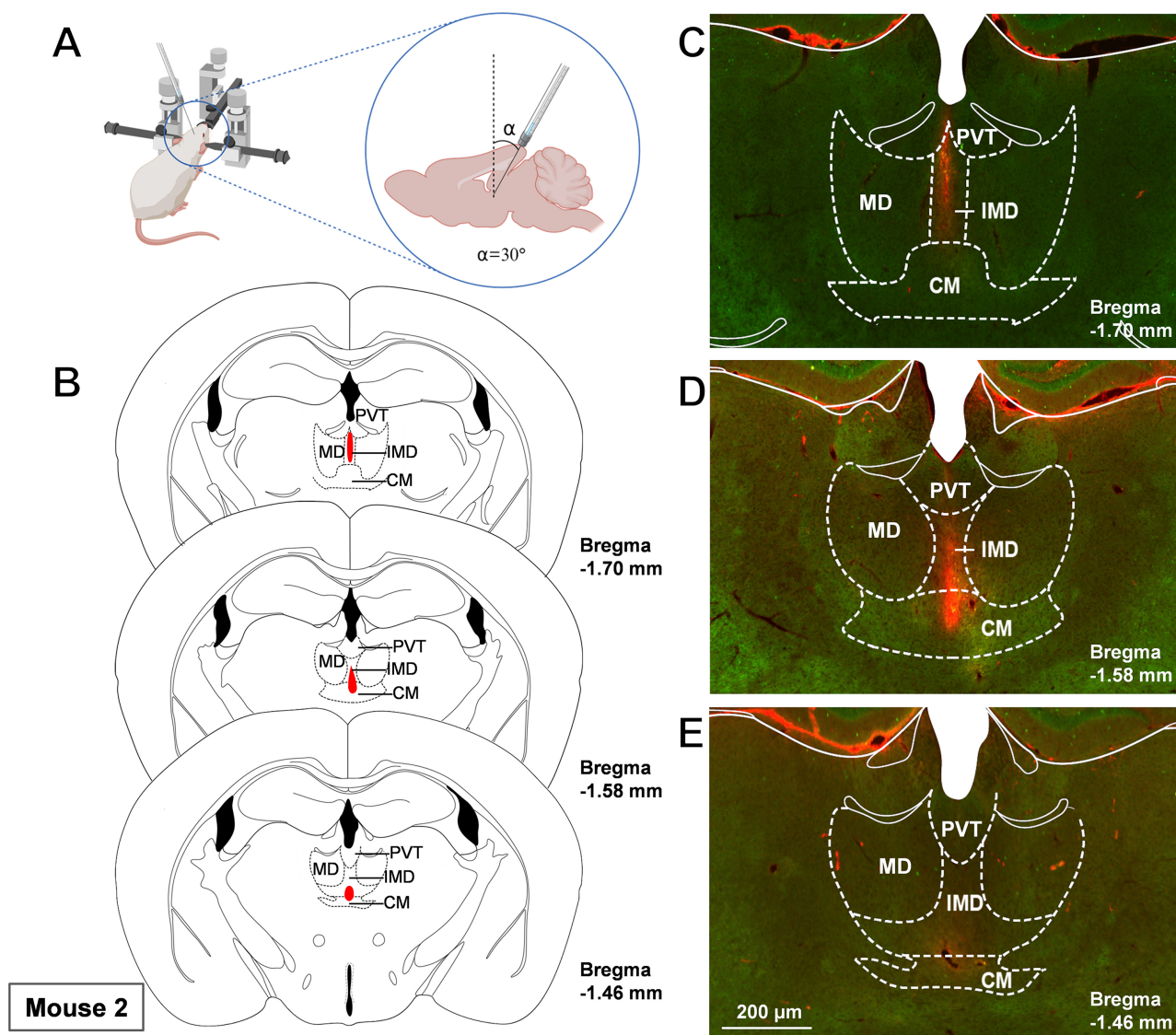


Fig. 1. CTB-Alexa 594 injection method and a schematic showing the injection sites in the MDTN. (A) The mouse was fixed on the stereotaxic frame, and the microinjector, which contained CTB-Alexa 594 tracing solution, was adjusted to lean back at a 30° angle to the vertical plane. The subsequent steps remain consistent with those of conventional injection. (B–E) The red regions indicate the CTB-Alexa 594 injection sites, involving the PVT, CM, and IMD of the MDTN in Mouse 2. The distances of the section from the bregma point are marked with different numbers. Scale bar = 200 μm. Abbreviations: CM, central medial thalamic nucleus; CTB, cholera toxin B subunit; IMD, intermediodorsal thalamic nucleus; MD, mediodorsal thalamic nucleus; MDTN, midline dorsal thalamic nuclei; PVT, paraventricular thalamic nucleus.

Sections from the second dish were incubated with 10% normal donkey serum (D9663, Sigma-Aldrich) for 30 min, followed by 3 washes with 0.01 M PBS (pH 7.4) for 10 min each. The sections were subsequently incubated with a mixture of goat anti-CTB (1:400; ab35988, Abcam, Cambridge, UK) and rabbit anti-GFP (1:500; A11122, Invitrogen) antibodies for 48 h at 4 °C. The sections were subsequently incubated with a mixture of Alexa 488 donkey anti-rabbit (1:500; A21206, Invitrogen) and Alexa 594 donkey anti-goat (1:500; A11058, Invitrogen) antibodies for 4–6 h at room temperature. Finally, the sections were mounted

onto clean glass slides, and sealed with PBS containing 50% glycerol (15514011, Invitrogen) and 2.5% triethylamine (HY-Y0566, MedChemExpress, Monmouth Junction, NJ, USA).

Sections from the third dish were mounted onto gelatin-coated glass slides (80312-3161, Citotest) and processed for Nissl staining to determine the location and boundary of the injection zone and brain structures.

Sections from the fourth dish were used as controls. A mixture of normal rabbit serum (NS01L, Sigma-Aldrich) and normal goat serum (S26F-MLSG, Sigma-Aldrich) was

used to replace the rabbit anti-GFP and goat anti-CTB to incubate the sections. The following procedures were the same as those used for the second serial sections. No positive staining was observed for the replaced antibodies.

To verify the specificity of labeled neurons in GAD67-GFP mice and the reliability of CTB as a retrograde tracer, we conducted two supplementary experiments. For the first experiment, immunofluorescence histochemical staining was performed on brain sections of GAD67-GFP mice. The antibodies used were rat-anti-GAD (1:200; OB-PRT084, Asis Biofarm, Hangzhou, Zhejiang, China) and Alexa 594 donkey anti-rat (1:400; A11007, Invitrogen). For the second experiment, Fluoro-Gold (FG) (39286, Sigma-Aldrich) was injected into the MDTN of GAD67-GFP mice in the same manner. Seven days after injection, brain sections were prepared, followed by immunofluorescence histochemical staining. The antibodies used were rabbit anti-FG (1:400; AB153-I, Sigma-Aldrich) and Alexa 594 goat anti-rabbit (1:400; ab150080, Abcam). The specific experimental procedures were consistent with those described above.

2.5 Image Acquisition and Data Analysis

Images were acquired via a confocal laser scanning microscope system (FV-1000, Olympus). To achieve proper separation of the signals, appropriate laser beams and filters were set as follows: Alexa 488 (excitation 488 nm, emission 500–530 nm) and Alexa 594 (excitation 543 nm, emission 590–615 nm). Digital images were captured via FLUOVIEW software (FV10-ASW 4.2, Olympus).

Cell counting of GAD67-GFP-immunoreactive (GAD^+), CTB retrograde-labeled (CTB^+), and GAD and CTB double-labeled (GAD^+CTB^+) neurons in every cortical region was performed on the second set of serial sections per mouse. ImageJ (version 1.54f; Wayne Rasband, National Institutes of Health, Bethesda, MD, USA; <https://imagej.net>) software was used to confirm the positively labeled neurons.

3. Results

3.1 Extent of the CTB-Alexa 594 Injection Site

To validate the specificity of GAD-GFP labeling in identifying GABAergic neurons, we performed immunofluorescence staining for GAD in the cerebral cortex of GAD-GFP mice. The majority of GFP^+ neurons were colocalized with GAD immunopositive neurons, confirming that the GAD-GFP mice specifically label cortical GABAergic neurons with high fidelity (**Supplementary Fig. 1**).

We injected CTB-Alexa 594 into the MDTN via an oblique needle trajectory to identify the cortical neurons projecting to the MDTN (Fig. 1A). Four mice (Mouse 2, 3, 5, and 8) that received accurate injections were selected for subsequent morphological observation and neuronal counting. A schematic of the CTB-Alexa 594 injection site (Mouse 2) in the MDTN is shown in Fig. 1B–E. A dense

core of the tracer was encircled by a diffuse halo at the injection site. The luminous area was considered the primary injection site. The extent of CTB-Alexa 594 diffusion in different coronal sections was determined on the basis of the stereotaxic coordinates [22] of adjacent sections.

GAD^+ , CTB^+ , and GAD^+CTB^+ neurons were distributed in the cerebral cortex. The GAD^+ neurons emitted green fluorescence, the CTB^+ neurons exhibited uniform red fluorescence in the perikarya, and the GAD^+CTB^+ neurons emitted both green fluorescence in the somata and red fluorescence in the perikarya.

3.2 Laminar Distribution of GAD^+ Neurons in the Cerebral Cortex

GAD^+ neurons are widely observed in the cerebral cortex. The primary motor cortex (M1), secondary motor cortex (M2) and orbitofrontal cortex (OFC) had the highest GAD^+ neurons density in layers V/VI, which contrasts with the minimal distribution in layer I. Within the primary somatosensory cortex (S1) and secondary somatosensory cortex (S2), layers II/III presented a greater density of GAD^+ neurons than the other layers did, whereas layer IV presented the sparsest distribution. The granular insula (GI) and dysgranular insula (DI) cortices displayed a high density of GAD^+ neurons in layers II/III, with comparable densities across the remaining layers. In the agranular insula cortex (AI), GAD^+ neurons are mainly distributed in the middle pyramidal layer. In the cingulate cortex (Cg) and prelimbic cortex (PrL), GAD^+ neurons exhibited a peak density in layers II/III and V, with the lowest density in layer I. A generally sparse distribution of GAD^+ neurons was observed in the piriform cortex (Pir) and claustrum (CL) (Fig. 2).

3.3 Distribution of CTB^+ Neurons in the Cerebral Cortex

CTB^+ neurons are predominantly distributed in the forebrain cortex, especially the M1, M2, OFC and limbic-associated cortical areas, including the Cg, PrL and insular cortex (AI and GI/DI). The CL, S1, S2 and Pir contained relatively lower proportions. More than 90% of the CTB^+ neurons were localized within deep layers (V–VI) of these cortical regions, with only minimal presence observed in layer IV of the S1 and S2 (Fig. 2).

3.4 Identification of GAD^+ Neurons in the Cerebral Cortex that Directly Project to the MDTN

The results showed that sparse GAD^+CTB^+ neurons were predominantly located in the M1, M2, S1, S2, GI/DI and AI cortices (Mouse 2, 3, 5, and 8). Fewer GAD^+CTB^+ neurons were observed in the OFC (Mouse 2 and 8), PrL (Mouse 2), and Cg (Mouse 3) (Fig. 2). No significant difference was observed between the left and right hemispheres. The somata were distributed mainly in layers V and VI of the S1, S2, M1, M2, GI/DI and in the middle

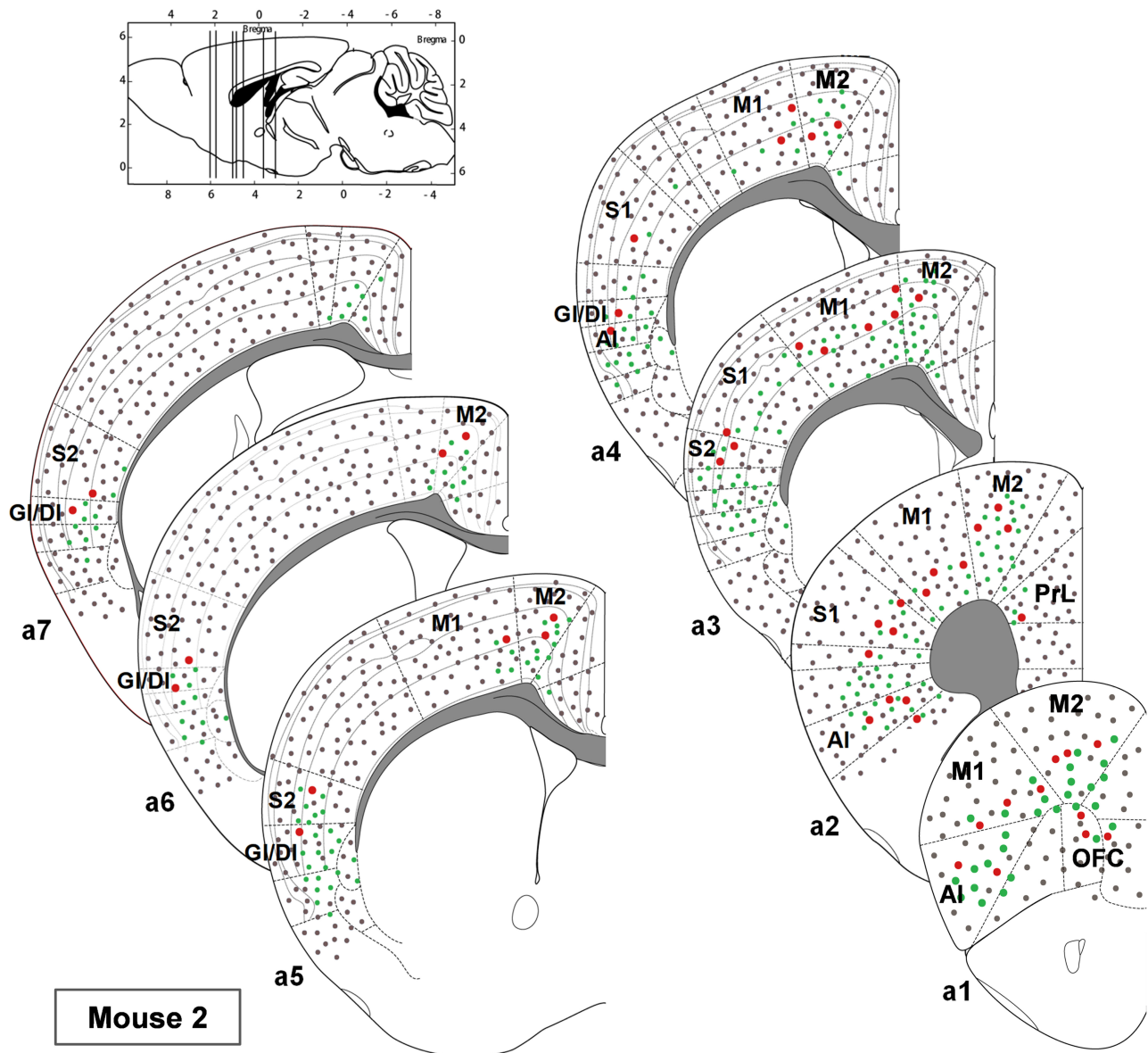


Fig. 2. Distribution of GAD^+ neurons, CTB^+ neurons, and GAD^+CTB^+ neurons in the cerebral cortex. Dots of different colors, representing GAD^+ neurons (gray), CTB^+ neurons (green), and GAD^+CTB^+ neurons (red), respectively, indicate their approximate distributions across different regions and layers of the cerebral cortex in Mouse 2. a1–7 represent different coronal planes of the brain of Mouse 2. Abbreviations: AI, agranular insular cortex; DI, dysgranular insular cortex; GAD, glutamic acid decarboxylase; CTB, cholera toxin B subunit; GI, granular insular cortex; M1, primary motor cortex; M2, secondary motor cortex; OFC, orbitofrontal cortex; PrL, prelimbic cortex; S1, primary somatosensory cortex; S2, secondary somatosensory cortex.

pyramidal layer of the AI, with all GAD^+CTB^+ neurons situated between -0.46 mm and $+2.34$ mm from bregma (Fig. 2).

The subsequent quantification of GAD^+ , CTB^+ , and GAD^+CTB^+ neurons within S1, S2, M1, M2, GI/DI, AI, OFC, PrL, Cg, CL and Pir were performed separately in 4 mice (Mouse 2, 3, 5, and 8). The percentages of GAD^+CTB^+ neurons to total GAD^+ and CTB^+ neurons in these cortical regions ranged from 0.25%–0.55% and 2.52%–4.93%, respectively. Furthermore, a detailed analysis of the proportion of GAD^+CTB^+ neurons to

CTB^+ neurons from these cortical regions showed that the highest proportion was in S1 (9.09%–15.25%), followed by M1 (4.27%–11.59%), GI/DI (2.02%–12.68%), AI (4.12%–5.20%), S2 (2.63%–7.45%), M2 (1.37%–3.36%), and OFC (0.00%–4.85%). Relatively small proportions of GAD^+CTB^+ neurons were observed in the PrL and Cg (Fig. 3 and Table 1).

To further verify the distribution pattern of cortical neurons projecting to the MDTN, we utilized Fluoro-Gold (FG) retrograde tracing as a complementary method to CTB. GAD^+ neurons in cortical areas exhibited colocaliza-

Table 1. The numbers of GAD⁺ neurons, CTB⁺ neurons, and GAD⁺+CTB⁺ neurons in different cortical regions of 4 mice (Mouse 2, 3, 5, and 8), and the proportions of GAD⁺+CTB⁺ neurons among the GAD⁺ and CTB⁺ neurons^a.

		S1	M1	GI/DI	AI	S2	M2	OFC	PrL	Cg	CL	Pir	Total
Mouse 2	GAD ⁺ neurons	6740	6560	690	1130	950	4640	4200	660	1120	630	1060	28,380
	CTB ⁺ neurons	22	515	63	97	94	899	206	130	166	90	10	2292
	GAD ⁺ +CTB ⁺ neurons	2	22	6	4	7	15	10	6	0	0	0	72
	GAD ⁺ +CTB ⁺ /GAD ⁺ (%)	0.03	0.34	0.87	0.35	0.74	0.32	0.24	0.91	0.00	0.00	0.00	0.25
	GAD ⁺ +CTB ⁺ /CTB ⁺ (%)	9.09	4.27	9.52	4.12	7.45	1.67	4.85	4.62	0.00	0.00	0.00	3.14
Mouse 3	GAD ⁺ neurons	6520	6610	700	1320	1020	4020	3990	590	1280	670	980	27,700
	CTB ⁺ neurons	78	578	56	93	85	1112	271	157	187	121	0	2738
	GAD ⁺ +CTB ⁺ neurons	11	67	6	4	3	23	0	0	4	0	0	114
	GAD ⁺ +CTB ⁺ /GAD ⁺ (%)	0.17	1.01	0.86	0.30	0.29	0.57	0.00	0.00	0.31	0.00	0.00	0.41
	GAD ⁺ +CTB ⁺ /CTB ⁺ (%)	14.10	11.59	10.71	4.30	3.53	2.07	0.00	0.00	2.14	0.00	0.00	4.16
Mouse 5	GAD ⁺ neurons	5990	5590	670	1270	1020	5030	3990	560	1300	660	1020	27,100
	CTB ⁺ neurons	59	611	99	145	76	1020	242	106	212	133	0	2703
	GAD ⁺ +CTB ⁺ neurons	9	35	2	6	2	14	0	0	0	0	0	68
	GAD ⁺ +CTB ⁺ /GAD ⁺ (%)	0.15	0.63	0.30	0.47	0.20	0.28	0.00	0.00	0.00	0.00	0.00	0.25
	GAD ⁺ +CTB ⁺ /CTB ⁺ (%)	15.25	5.73	2.02	4.14	2.63	1.37	0.00	0.00	0.00	0.00	0.00	2.52
Mouse 8	GAD ⁺ neurons	6770	5830	750	1450	880	4470	3830	620	1170	710	990	27,470
	CTB ⁺ neurons	77	704	71	173	44	1311	189	139	191	140	6	3045
	GAD ⁺ +CTB ⁺ neurons	10	69	9	9	2	44	7	0	0	0	0	150
	GAD ⁺ +CTB ⁺ /GAD ⁺ (%)	0.15	1.18	1.20	0.62	0.23	0.98	0.18	0.00	0.00	0.00	0.00	0.55
	GAD ⁺ +CTB ⁺ /CTB ⁺ (%)	12.99	9.80	12.68	5.20	4.55	3.36	3.70	0.00	0.00	0.00	0.00	4.93
Average	GAD ⁺ neurons	6505	6147.5	702.5	1292.5	967.5	4540	4002.5	607.5	1217.5	667.5	1012.5	27,662.5
	CTB ⁺ neurons	59	602	72.25	122	74.75	1085.5	227	140.5	189	121	33.5	2726.5
	GAD ⁺ +CTB ⁺ neurons	8	48.25	5.75	5.75	3.5	24	4.25	1.5	1	0	0	100
	GAD ⁺ +CTB ⁺ /GAD ⁺ (%)	0.12	0.78	0.39	0.44	0.36	0.53	0.10	0.25	0.08	0.00	0.00	0.36
	GAD ⁺ +CTB ⁺ /CTB ⁺ (%)	13.56	8.02	7.96	4.71	4.68	2.21	1.87	1.07	0.53	0.00	0.00	3.67

^aCell counting was performed on the second section of every fourth serial section. Abbreviations: Cg, cingulate cortex; CL, claustrum; Pir, piriform cortex.

tion with FG⁺ neurons, and the distribution of these double-labeled neurons was consistent with that observed in CTB tracing results (**Supplementary Fig. 2**).

3.5 Morphological Characteristics of GAD⁺ Neurons Projecting From the Cerebral Cortex to the MDTN

The morphological features of GAD⁺+CTB⁺ neurons across the S1, S2, M1, M2, GI/DI, AI, OFC, Cg, and PrL were observed. Notably, the GAD⁺+CTB⁺ neurons mainly distributed in the deep layers of the sensory, motor, and insular cortices. In contrast, the CL and Pir exhibited a distribution of only GAD⁺ neurons and CTB⁺ neurons, with the absence of GAD⁺+CTB⁺ neurons. The majority of GAD⁺+CTB⁺ neurons were small multipolar neurons with polygonal, round, or oval somata (15–25 μ m in diameter) (Fig. 4).

4. Discussion

The present results showed that GAD⁺+CTB⁺ neurons were predominantly localized in the M1, M2, S1, and insular cortex (IC). Fewer of them were observed in the

OFC, PrL, and Cg. The results confirmed the existence of the long-range GABAergic projections from the cortex to the MDTN.

Cortical GABAergic neurons project to multiple subcortical structures. GABAergic neurons from the auditory and motor cortices innervate the dorsal striatum and suppress the output of spiny projection neurons (SPNs), potentially fine-tuning motor programs and habit learning by precisely controlling the timing and firing rates of SPNs [23,24]. Additionally, auditory cortical GABAergic neurons send long-range inhibitory projections to the amygdala, thereby modulating sound-driven aversive or fear behaviors [25]. The cortex also dispatches GABAergic projections to other subcortical targets including the thalamus, superior colliculus, inferior colliculus, and olfactory bulb [26]. Notably, there is a lack of systematic morphological studies on corticothalamic inhibitory connections.

Corticothalamic interconnections constitute fundamental neural pathways for modulating cognition, emotion, pain and itch sensation [27,28]. As a pivotal component of the “limbic thalamus” [29], the MDTN is a key hub for sensory integration and emotional regulation. Clarifying the

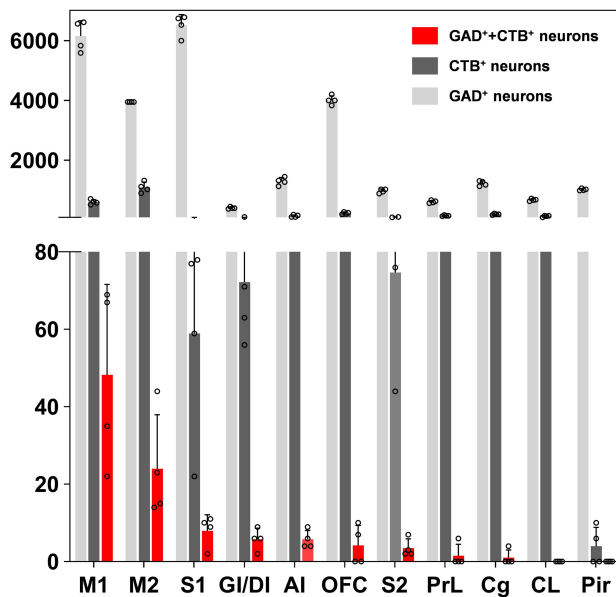


Fig. 3. Numbers of GAD⁺ neurons, CTB⁺ neurons, and GAD⁺CTB⁺ neurons in different cortical regions of 4 mice (Mouse 2, 3, 5, and 8). The quantification of GAD⁺ neurons, CTB⁺ neurons, and GAD⁺CTB⁺ neurons in each cortical region of 4 mice (Mouse 2, 3, 5, and 8) was conducted, and the number of GAD⁺CTB⁺ neurons was ranked in descending order. Each small circle in the bar graph represents the count of this type of neuron in each brain region from a single mouse.

anatomical connections of the cortex-MDTN pathway as well as associated functions is highly important. The functions exerted by GABAergic projections from different cortical regions to the MDTN may differ.

In the motor cortex, the role of LRGNs in filtering extraneous movement signals is crucial for motor output precision. As the primary region for planning, controlling, and executing voluntary movements, the motor cortex requires effective suppression of competing motor plans during the preparation phases [30]. Our observation of LRGNs distributed in the M1 and M2 suggested potential selection processes through thalamic inhibition. The well-characterized cortico-basal ganglia-thalamic pathway, which is essential for motor control, involves similar long-range inhibitory projections [31]. The newly identified inhibitory projections from the motor cortex to the MDTN may constitute a parallel pathway for motor command refinement, selectively gating appropriate movement signals.

In the sensory cortex, the S1 receives direct thalamic inputs from specific sensory nuclei and is responsible for the accuracy of sensory information and spatial detail. According to the present research, the LRGNs in S1 may amplify salient stimuli by suppressing redundant information. This mechanism is consistent with findings in the olfactory system, where corticofugal inhibitory projections from the olfactory cortex dynamically modulate sensory processing

in the lateral hypothalamus [32]. We also observed that there are fewer LRGNs in S2 than in S1, because S2 that receives information from S1 and is responsible for further processes of sensory information [33]. The sensory cortex-MDTN inhibitory pathway likely represents a comparable top-down control system for sensory information prioritization.

The IC integrates visceral and somatic sensory information and is connected to limbic structures involved in emotional processing, such as the amygdala [34]. The IC plays a pivotal role in the experience of emotions related to bodily states [35]. Inhibitory projections from the IC to the MDTN in the present research could filter out redundant sensory signals, thereby preventing overactivation of the emotional response system.

The OFC receives inputs from multiple sensory and limbic areas and is involved in a variety of functions related to emotional and cognitive processing. The role of the OFC in outcome valuation and adaptive representation updating has been previously demonstrated [36]. According to the current morphological results, the inhibitory action of LRGNs in the OFC could help fine-tune this process, ensuring rational and appropriate decision-making.

The PrL is a key part of the medial prefrontal cortex and is involved in cognitive flexibility, fear extinction, and goal-directed behavior [37]. In the present research, LRGNs in the PrL projecting to the MDTN were observed in only one mouse (Mouse 2). The sparse presence of these inhibitory projections suggests that they may regulate cognition and emotion by inhibiting thalamic nuclei, which requires functional validation.

The Cg, which is divided into the anterior cingulate cortex (ACC) and posterior subregions, is involved in pain processing, error monitoring, and emotional salience detection [38]. Our previous research indicated that the ACC facilitates pain through ACC-spinal cord excitatory projecting neurons in a top-down manner [39]. Only few inhibitory projections from the Cg to the MDTN were observed in the present study, suggesting that these projections may play only an auxiliary role rather than excitatory projection neurons.

As demonstrated in the study by Tomioka *et al.* [11], GABAergic neurons in the cerebral cortex that project to the striatum are predominantly distributed in layers II/III and V, whereas those projecting to the mediodorsal thalamic nucleus are mainly localized in layer VI. These laminar distribution characteristics are consistent with the findings of the present study.

Cortical GABAergic neurons mediate both local and long-range neural modulation through “disinhibition” and “synchronization” mechanisms [40]. Although LRGNs represent a relatively small subpopulation of cortical GABAergic neurons, their synaptic connectivity patterns reveal a functionally significant organization. Recent study determining presynaptic and postsynaptic neuronal identi-

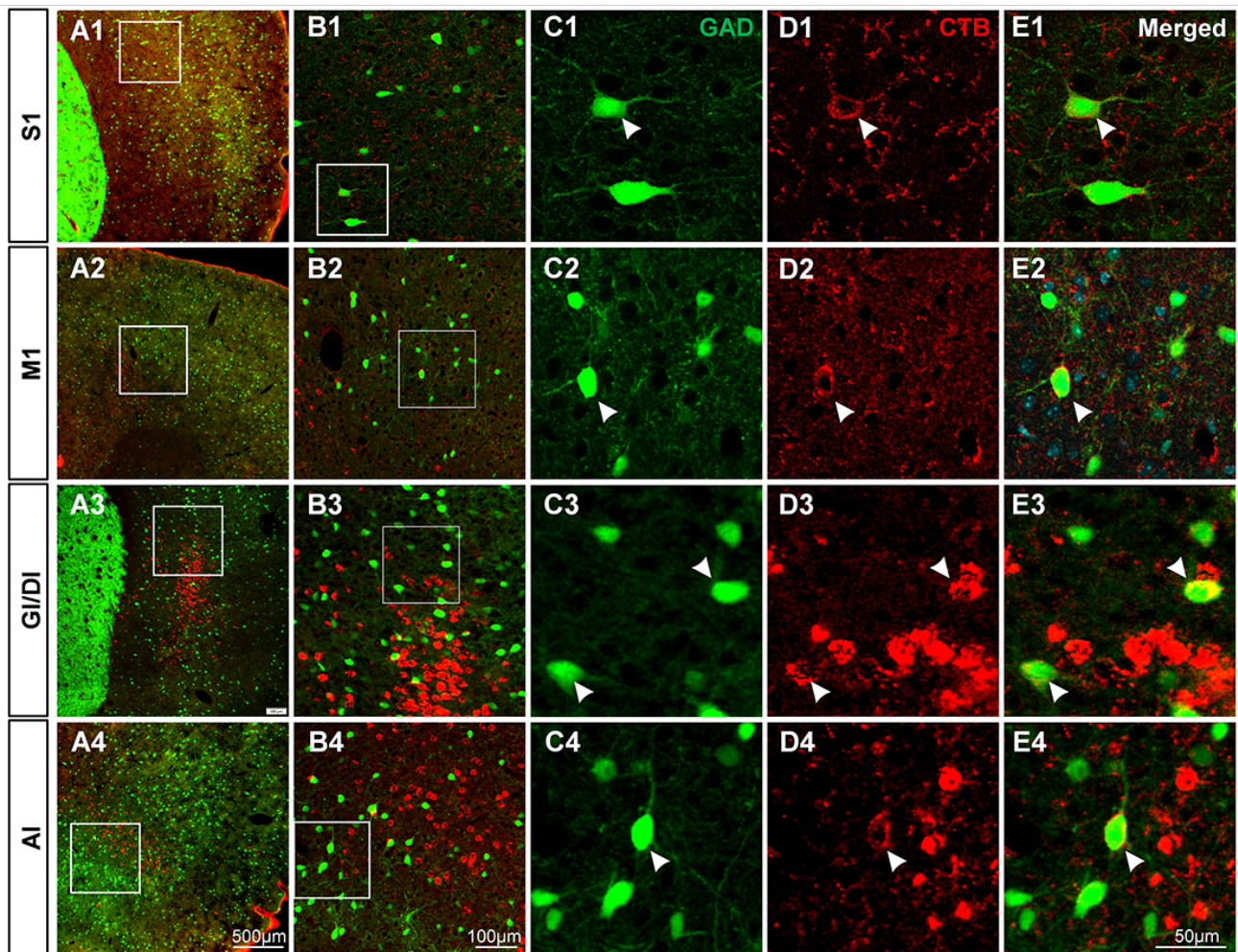


Fig. 4. Distribution of GAD⁺ neurons, CTB⁺ neurons and GAD⁺+CTB⁺ neurons in different cortical regions. GAD⁺+CTB⁺ neurons were mainly observed in the S1, M1, GI/DI, and AI in 4 mice (Mouse 2, 3, 5, and 8). The white rectangular regions in A1–A4 are magnified in B1–B4. The white rectangular regions in B1–B4 are further enlarged to display in C1–C4, D1–D4 and E1–E4. GAD⁺ neurons are shown in green, and CTB⁺ neurons are shown in red. The white triangles indicate GAD⁺+CTB⁺ neurons. Scale bar = 500 μ m (A1–A4), 100 μ m (B1–B4), and 50 μ m (C1–C4, D1–D4 and E1–E4).

ties have demonstrated that cortical LRGNs predominantly target inhibitory interneurons rather than excitatory neurons [12], suggesting that disinhibition pathways are the primary mode of action. Previous studies have demonstrated that individual cortical GABAergic neurons typically exhibit divergent projections to multiple brain regions [41,42]. The cortical LRGNs might exhibit broad connectivity patterns. In addition to the MDTN, cortical LRGNs may also project simultaneously to other brain regions, thereby exerting a synergistic effect on multiple neural functions.

5. Conclusions

The present study provides definitive anatomical evidence of direct GABAergic corticothalamic projections to the MDTN. We propose that they may serve as crucial modulators of thalamic information processing, potentially influencing sensory transmission, motor control, and

emotional regulation at the thalamic level. This GABAergic pathway may represent a previously underappreciated mechanism for the cortical regulation of thalamic function. Last but not least, it's necessary to check whether the conclusion is consistent in females. Further investigation is certainly needed to clarify the gender differences and functional characteristics of this long-range inhibitory projections in the future.

Availability of Data and Materials

All data reported in this paper will be shared by the lead contact upon request.

Author Contributions

YQL and MMZ designed the study and edited the manuscript; YYL and FL conducted the experiments and the data analysis; YYL performed the cell counts. FL pro-

vided language modifications. All authors contributed to editorial changes in the manuscript. All authors read and approved the final manuscript. All authors have participated sufficiently in the work and agreed to be accountable for all aspects of the work.

Ethics Approval and Consent to Participate

All animal experiments were conducted in accordance with the Fourth Military Medical University Guide for the Use of Laboratory Animals and approved by the Fourth Military Medical University Ethics Committee (protocol No. 20211018, Xi'an, China).

Acknowledgment

Not applicable.

Funding

This work was supported by grants from the STI2030-Major Projects (No. 2021ZD0204403 to Y.-Q. Li and M.-M. Zhang) and the National Natural Science Foundation of China (Nos. 82130034, 82221001 and 82471254 to Y.-Q. Li; No. 82371246 to M.-M. Zhang).

Conflict of Interest

The authors declare no conflict of interest.

Supplementary Material

Supplementary material associated with this article can be found, in the online version, at <https://doi.org/10.31083/JIN47187>.

References

- [1] Larkum ME, Petro LS, Sachdev RNS, Muckli L. A Perspective on Cortical Layering and Layer-Spanning Neuronal Elements. *Frontiers in Neuroanatomy*. 2018; 12: 56. <https://doi.org/10.3389/fnana.2018.00056>.
- [2] Song Q, Wei A, Xu H, Gu Y, Jiang Y, Dong N, *et al.* An ACC-VTA-ACC positive-feedback loop mediates the persistence of neuropathic pain and emotional consequences. *Nature Neuroscience*. 2024; 27: 272–285. <https://doi.org/10.1038/s41593-023-01519-w>.
- [3] Lewis EM, Spence HE, Akella N, Buonanno A. Pathway-specific contribution of parvalbumin interneuron NMDARs to synaptic currents and thalamocortical feedforward inhibition. *Molecular Psychiatry*. 2022; 27: 5124–5134. <https://doi.org/10.1038/s41380-022-01747-9>.
- [4] Liang J, Yang Z, Zhou C. Excitation-Inhibition Balance, Neural Criticality, and Activities in Neuronal Circuits. *The Neuroscientist: a Review Journal Bringing Neurobiology, Neurology and Psychiatry*. 2025; 31: 31–46. <https://doi.org/10.1177/10738584231221766>.
- [5] Wen W, Turrigiano GG. Keeping Your Brain in Balance: Homeostatic Regulation of Network Function. *Annual Review of Neuroscience*. 2024; 47: 41–61. <https://doi.org/10.1146/annurev-neuro-092523-110001>.
- [6] Urrutia-Piñones J, Morales-Moraga C, Sanguinetti-González N, Escobar AP, Chiu CQ. Long-Range GABAergic Projections of Cortical Origin in Brain Function. *Frontiers in Systems Neuroscience*. 2022; 16: 841869. <https://doi.org/10.3389/fnsys.2022.841869>.
- [7] Code RA, Winer JA. Commissural neurons in layer III of cat primary auditory cortex (AI): pyramidal and non-pyramidal cell input. *The Journal of Comparative Neurology*. 1985; 242: 485–510. <https://doi.org/10.1002/cne.902420404>.
- [8] Totterdell S, Hayes L. Non-pyramidal hippocampal projection neurons: a light and electron microscopic study. *Journal of Neurocytology*. 1987; 16: 477–485. <https://doi.org/10.1007/BF01668502>.
- [9] Naskar S, Qi J, Pereira F, Gerfen CR, Lee S. Cell-type-specific recruitment of GABAergic interneurons in the primary somatosensory cortex by long-range inputs. *Cell Reports*. 2021; 34: 108774. <https://doi.org/10.1016/j.celrep.2021.108774>.
- [10] Melzer S, Gil M, Koser DE, Michael M, Huang KW, Monyer H. Distinct Corticostriatal GABAergic Neurons Modulate Striatal Output Neurons and Motor Activity. *Cell Reports*. 2017; 19: 1045–1055. <https://doi.org/10.1016/j.celrep.2017.04.024>.
- [11] Tomioka R, Sakimura K, Yanagawa Y. Corticofugal GABAergic projection neurons in the mouse frontal cortex. *Frontiers in Neuroanatomy*. 2015; 9: 133. <https://doi.org/10.3389/fnana.2015.00133>.
- [12] Mazo C, Nissant A, Saha S, Peroni E, Lledo PM, Lepousez G. Long-range GABAergic projections contribute to cortical feedback control of sensory processing. *Nature Communications*. 2022; 13: 6879. <https://doi.org/10.1038/s41467-022-34513-0>.
- [13] Harris JA, Mihalas S, Hirokawa KE, Whitesell JD, Choi H, Bernard A, *et al.* Hierarchical organization of cortical and thalamic connectivity. *Nature*. 2019; 575: 195–202. <https://doi.org/10.1038/s41586-019-1716-z>.
- [14] Ren S, Wang Y, Yue F, Cheng X, Dang R, Qiao Q, *et al.* The paraventricular thalamus is a critical thalamic area for wakefulness. *Science (New York, N.Y.)*. 2018; 362: 429–434. <https://doi.org/10.1126/science.aat2512>.
- [15] Kirouac GJ. Update on the connectivity of the paraventricular nucleus of the thalamus and its position within limbic corticostriatal circuits. *Neuroscience and Biobehavioral Reviews*. 2025; 169: 105989. <https://doi.org/10.1016/j.neubiorev.2024.105989>.
- [16] Liang SH, Zhao WJ, Yin JB, Chen YB, Li JN, Feng B, *et al.* A Neural Circuit from Thalamic Paraventricular Nucleus to Central Amygdala for the Facilitation of Neuropathic Pain. *The Journal of Neuroscience*. 2020; 40: 7837–7854. <https://doi.org/10.1523/JNEUROSCI.2487-19.2020>.
- [17] Dong P, Wang H, Shen XF, Jiang P, Zhu XT, Li Y, *et al.* A novel cortico-intrathalamic circuit for flight behavior. *Nature Neuroscience*. 2019; 22: 941–949. <https://doi.org/10.1038/s41593-019-0391-6>.
- [18] Li JN, Wu XM, Zhao LJ, Sun HX, Hong J, Wu FL, *et al.* Central medial thalamic nucleus dynamically participates in acute itch sensation and chronic itch-induced anxiety-like behavior in male mice. *Nature Communications*. 2023; 14: 2539. <https://doi.org/10.1038/s41467-023-38264-4>.
- [19] Cacciatori M, Magnani FG, Barbadoro F, Ippoliti C, Stanziano M, Clementi L, *et al.* Thalamus and consciousness: a systematic review on thalamic nuclei associated with consciousness. *Frontiers in Neurology*. 2025; 16: 1509668. <https://doi.org/10.3389/fneur.2025.1509668>.
- [20] Lee SE, Lee Y, Lee GH. The regulation of glutamic acid decarboxylases in GABA neurotransmission in the brain. *Archives of Pharmacological Research*. 2019; 42: 1031–1039. <https://doi.org/10.1007/s12272-019-01196-z>.
- [21] Wang S, Deng Z, Wang J, Zhang W, Liu F, Xu J, *et al.* Decreased GABAergic signaling, fewer parvalbumin-, somatostatin- and calretinin-positive neurons in brain of a rat model of simulated transport stress. *Research in Veterinary Science*. 2021; 134: 86–95. <https://doi.org/10.1016/j.rvsc.2020.12.005>.

- [22] Paxinos G, Franklin KBJ. Paxinos and Franklin's the Mouse Brain in Stereotaxic Coordinates. 5th edn. Academic Press: San Diego. 2019.
- [23] Rock C, Zurita H, Wilson C, Apicella AJ. An inhibitory cortico-striatal pathway. *eLife*. 2016; 5: e15890. <https://doi.org/10.7554/eLife.15890>.
- [24] Bertero A, Zurita H, Normandin M, Apicella AJ. Auditory Long-Range Parvalbumin Cortico-Striatal Neurons. *Frontiers in Neural Circuits*. 2020; 14: 45. <https://doi.org/10.3389/fncir.2020.00045>.
- [25] Bertero A, Feyen PLC, Zurita H, Apicella AJ. A Non-Canonical Cortico-Amygdala Inhibitory Loop. *The Journal of Neuroscience*. 2019; 39: 8424–8438. <https://doi.org/10.1523/JNEUROSCI.1515-19.2019>.
- [26] Bertero A, Garcia C, Apicella AJ. Corticofugal VIP Gabaergic Projection Neurons in the Mouse Auditory and Motor Cortex. *Frontiers in Neural Circuits*. 2021; 15: 714780. <https://doi.org/10.3389/fncir.2021.714780>.
- [27] Shih HC, Kuan YH, Shyu BC. Targeting brain-derived neurotrophic factor in the medial thalamus for the treatment of central poststroke pain in a rodent model. *Pain*. 2017; 158: 1302–1313. <https://doi.org/10.1097/j.pain.0000000000000915>.
- [28] Zhang SR, Wu DY, Luo R, Wu JL, Chen H, Li ZM, *et al*. A Prelimbic Cortex-Thalamus Circuit Bidirectionally Regulates Innate and Stress-Induced Anxiety-Like Behavior. *The Journal of Neuroscience*. 2024; 44: e2103232024. <https://doi.org/10.1523/JNEUROSCI.2103-23.2024>.
- [29] Vertes RP, Linley SB, Hoover WB. Limbic circuitry of the midline thalamus. *Neuroscience and Biobehavioral Reviews*. 2015; 54: 89–107. <https://doi.org/10.1016/j.neubiorev.2015.01.014>.
- [30] Svoboda K, Li N. Neural mechanisms of movement planning: motor cortex and beyond. *Current Opinion in Neurobiology*. 2018; 49: 33–41. <https://doi.org/10.1016/j.conb.2017.10.023>.
- [31] Foster NN, Barry J, Korobkova L, Garcia L, Gao L, Baccerra M, *et al*. The mouse cortico-basal ganglia-thalamic network. *Nature*. 2021; 598: 188–194. <https://doi.org/10.1038/s41586-021-03993-3>.
- [32] Murata K, Kinoshita T, Fukazawa Y, Kobayashi K, Kobayashi K, Miyamichi K, *et al*. GABAergic neurons in the olfactory cortex projecting to the lateral hypothalamus in mice. *Scientific Reports*. 2019; 9: 7132. <https://doi.org/10.1038/s41598-019-43580-1>.
- [33] Kropf E, Syan SK, Minuzzi L, Frey BN. From anatomy to function: the role of the somatosensory cortex in emotional regulation. *Revista Brasileira De Psiquiatria (Sao Paulo, Brazil: 1999)*. 2019; 41: 261–269. <https://doi.org/10.1590/1516-4446-2018-0183>.
- [34] Chen J, Gao Y, Bao ST, Wang YD, Jia T, Yin C, *et al*. Insula→Amygdala and Insula→Thalamus Pathways Are Involved in Comorbid Chronic Pain and Depression-Like Behavior in Mice. *The Journal of Neuroscience*. 2024; 44: e2062232024. <https://doi.org/10.1523/JNEUROSCI.2062-23.2024>.
- [35] Li F, Li ZA, Li J, Tian HM, Li DN, Liu ZY, *et al*. Projection from the parafascicular nucleus of the thalamus to the insular cortex mediate analgesia and anti-anxiety behaviors in mice. *Neurobiology of Disease*. 2025; 216: 107107. <https://doi.org/10.1016/j.nbd.2025.107107>.
- [36] Oyama K, Majima K, Nagai Y, Hori Y, Hirabayashi T, Eldridge MAG, *et al*. Distinct roles of monkey OFC-subcortical pathways in adaptive behavior. *Nature Communications*. 2024; 15: 6487. <https://doi.org/10.1038/s41467-024-50505-8>.
- [37] Zeidler Z, DeNardo L. The Role of Prefrontal Ensembles in Memory Across Time: Time-Dependent Transformations of Prefrontal Memory Ensembles. *Advances in Neurobiology*. 2024; 38: 67–78. https://doi.org/10.1007/978-3-031-62983-9_5.
- [38] Shi W, Xue M, Wu F, Fan K, Chen QY, Xu F, *et al*. Whole-brain mapping of efferent projections of the anterior cingulate cortex in adult male mice. *Molecular Pain*. 2022; 18: 17448069221094529. <https://doi.org/10.1177/17448069221094529>.
- [39] Chen T, Taniguchi W, Chen QY, Tozaki-Saitoh H, Song Q, Liu RH, *et al*. Top-down descending facilitation of spinal sensory excitatory transmission from the anterior cingulate cortex. *Nature Communications*. 2018; 9: 1886. <https://doi.org/10.1038/s41467-018-04309-2>.
- [40] Bocchio M, Vorobyev A, Sadeh S, Brustlein S, Dard R, Reichinek S, *et al*. Functional networks of inhibitory neurons orchestrate synchrony in the hippocampus. *PLoS Biology*. 2024; 22: e3002837. <https://doi.org/10.1371/journal.pbio.3002837>.
- [41] Bollmann Y, Modol L, Tressard T, Vorobyev A, Dard R, Brustlein S, *et al*. Prominent in vivo influence of single interneurons in the developing barrel cortex. *Nature Neuroscience*. 2023; 26: 1555–1565. <https://doi.org/10.1038/s41593-023-01405-5>.
- [42] Fuchs EC, Neitz A, Pinna R, Melzer S, Caputi A, Monyer H. Local and Distant Input Controlling Excitation in Layer II of the Medial Entorhinal Cortex. *Neuron*. 2016; 89: 194–208. <https://doi.org/10.1016/j.neuron.2015.11.029>.